entrainable oscillator. Note that the different rhythmic *frq* mutants show strain-specific responses to short light pulses[25,26].

In laboratory experiments, the effect of light on the *Neurospora* clock, even at moonlight levels, is so strong that it apparently stops the oscillator[22]. In nature, such a clock would be no more than an hourglass timer, functioning only during the darkest nights. The light-cycle experiments shown here were done in constant temperature, but when light and temperature are given in anti-phase in a 24 h cycle (cold with light and warm with dark)[20], temperature dominates as the *zeitgeber*. When frq^{+} is exposed to temperature cycles (22–27 °C) in constant light (which results in arrhythmicity in constant temperature), conidiation is robustly rhythmic (data not shown). Thus, temperature cycles 'gate' light transduction, enabling the *Neurospora* clock to continue throughout the day. Our results show that FRQ is unnecessary for entraining an oscillator with generic circadian properties in temperature cycles. However, without FRQ, the circadian clock cannot synchronize to light:dark cycles and self-sustained rhythmicity is almost never seen, except under special conditions[13,14,27]. As part of a circadianly regulated light input pathway[1–3], FRQ apparently supplies the clock with sufficient amplitude for self-sustained rhythmicity (frq^{9} remains arrhythmic after release from temperature entrainment) and sets the period in the circadian range. This role of FRQ is especially relevant in view of the recent reports of clock-regulated light transduction (via cryptochrome) to the clock in flies and mammals[1,28,29]. □

Methods

Strains and media. *bd*, *bd frq*^{1} and *bd frq*^{9} are standard lab strains (provided by the Dunlap Lab, Dartmouth Medical School). *bd frq*^{7} was obtained from the Fungal Genetics Stock Center. Solid media for glass tubes contained 1× Vogels salts[14], 0.3% glucose, 0.5% L-arginine, 2% agar and 10 ng biotin per ml. Liquid media was the same, except for 0.5% glucose and the lack of agar.

***Zeitgeber* cycles.** Depending on the *zeitgeber*, half of each cycle was spent in low temperature or darkness, the other half in high temperature or light (Lumilux Interna, Osram). Temperature cycles were created in custom-made incubators. For increases in temperature, 90% of the end point (22 to 27 °C) was attained in 48 min. For decreases (27 to 22 °C) 108 min was required for 90% of the change. Light cycles were administered at constant temperature (26 or 22 °C). Fluence was titrated with neutral density filters (Rosco). Glass tubes were inoculated and incubated for about 1 day in constant light and ambient lab temperature (23 ± 1 °C) before transfer to the *zeitgeber* cycle (low temperature or darkness).

mRNA analysis. Glass tubes and liquid cultures (3.7×10^{8} conidia per 10 ml of media, in a 50 ml Erlenmeyer flask) were simultaneously inoculated and transferred (see above) to the experimental set-up. Samples were collected over the course of the third full cycle, by which time conidiation rhythms are generally stably entrained. RNA was prepared and analysed by standard methods[12,21]. Loading differences were normalized by relating *frq* to ribosomal RNA. For each individual data set, the average quantification in the frq^{9} series is 1 and all other values (frq^{+} and frq^{9}) are expressed as proportions thereof.

Data analysis. Images of glass tubes were digitized with an Apple Color One scanner, stored as PICT files and analysed with CHRONO[30]. Conidiation was quantified by the number of white pixels in each vertical line of the image and expressed as deviation around the non-rhythmic trend. 3–6 tubes were analysed for each time series and variable. Onsets of conidiation were defined as upward transition through the non-rhythmic trend (see zero lines in Figs 2b and 4c) of the averaged time series.

Received 12 January; accepted 19 April 1999.

1. Emery, P., So, W V., Kaneko, M., Hall, J. C. & Rosbash, M. CRY, a Drosophila clock and light-regulated cryptochrome, is a major contributor to circadian rhythm resetting and photosensitivity. *Cell* **95,** 669–679 (1998).
2. Roenneberg, T. & Deng, T.-S. Photobiology of the *Gonyaulax* circadian system: I Different phase response curves for red and blue light. *Planta* **202,** 494–501 (1997).
3. Roenneberg, T. & Foster, R. G. Twilight times—light and the circadian system. *Photochem. Photobiol.* **66,** 549–561 (1997).
4. Block, G., Geusz, M., Khalsa, S., Michel, S. & Whitmore, D. (eds). *Cellular Analysis of a Molluscan Retinal Biological Clock* 51–66 (Wiley, Chichester, 1995).
5. Mrosovsky, N., Salmon, P. A., Menaker, M. & Ralph, M. R. Nonphotic phase shifting in hamster clock mutants. *J. Biol. Rhythms* **7,** 41–50 (1992).
6. Roenneberg, T. & Merrow, M. Molecular circadian oscillators—an alternative hypothesis. *J. Biol. Rhythms* **13,** 167–179 (1998).
7. Aschoff, J. (ed.) *Biological Rhythms* (Plenum, New York, 1981).
8. Aschoff, J. in *Proc. XIII Int. Conf. Soc. Chronobiol. (Pavia 1977)* (Halberg, F. *et al.*, eds) 105–112 (Il Ponte, Milan, 1981).
9. Bruce, V. Environmental entrainment of circadian rhythms. *Cold Spring Harbor Symp. Quant. Biol.* **25,** 29–48 (1960).
10. Aronson, B. D., Johnson, K. A., Loros, J. J. & Dunlap, J. C. Negative feedback defining a circadian clock: autoregulation of the clock gene *frequency*. *Science* **263,** 1578–1584 (1994).
11. Garceau, N. Y., Liu, Y., Loros, J. J. & Dunlap, J. Alternative initiation of translation and time specific phosphorylation yield multiple forms of essential clock protein FREQUENCY. *Cell* **89,** 469–476 (1997).
12. Crosthwaite, S. K., Loros, J. J. & Dunlap, J. C. Light-induced resetting of a circadian clock is mediated by a rapid increase in *frequency* transcript. *Cell* **81,** 1003–1012 (1995).
13. Loros, J. J. & Feldman, J. F. Loss of temperature compensation of circadian period length in the *frq*-9 mutant of *Neurospora crassa*. *J. Biol. Rhythms* **1,** 187–198 (1986).
14. Aronson, B. D., Johnson, K. A. & Dunlap, J. C. The circadian clock locus *frequency*: a single ORF defines period length and temperature compensation. *Proc. Natl Acad. Sci. USA* **91,** 7683–7687 (1994).
15. Feldman, J. F. & Hoyle, M. N. Isolation of circadian clock mutants of *Neurospora crassa*. *Genetics* **75,** 605–613 (1973).
16. Merrow, M. W. & Dunlap, J. C. Intergeneric complementation of a circadian rhythmicity defect: phylogenetic conservation of structure and function of the clock gene *frequency*. *EMBO J.* **13,** 2257–2266 (1994).
17. Somers, D. E., Webb, A. A., Pearson, M. & Kay, S. A. The short-period mutant, *toc1-1*, alters circadian clock regulation of multiple outputs throughout development in *Arabidopsis thaliana*. *Development* **125,** 485–494 (1998).
18. Crosthwaite, S. K., Dunlap, J. C. & Loros, J. J. *Neurospora wc-1* and *wc-2*: Transcription, photoresponses, and the origin of circadian rhythmicity. *Science* **276,** 763–769 (1997).
19. Russo, V. E. Blue light induces circadian rhythms in the *bd* mutant of *Neurospora*: double mutants *bd,wc-1* and *bd,wc-2* are blind. *J. Photochem. Photobiol. B* **2,** 59–65 (1988).
20. Liu, Y., Merrow, M., Loros, J. L. & Dunlap, J. C. How temperature changes reset a circadian oscillator. *Science* **281,** 825–829 (1998).
21. Merrow, M., Garceau, N. & Dunlap, J. Dissection of a circadian oscillation into discrete domains. *Proc. Natl Acad. Sci. USA* **94,** 3877–3882 (1997).
22. Sargent, M. L., Briggs, W. R. & Woodward, D. O. Circadian nature of a rhythm expressed by an invertaseless strain of *Neurospora crassa*. *Plant Physiol.* **41,** 1343–1349 (1956).
23. Winfree, A. T. Suppressing *Drosophila* circadian rhythm with dim light. *Science* **183,** 970–972 (1974).
24. Arpaia, G., Loros, J. J., Dunlap, J. C., Morelli, G. & Macino, G. The interplay of light and the circadian clock. *Plant Physiol.* **102,** 1299–1305 (1993).
25. Chang, B. & Nakashima, H. Effects of light-dark cycles on the circadian conidiation rhythm in *Neurospora crassa*. *J. Plant Res.* **110,** 449–453 (1997).
26. Dharmananda, S. *Studies of the Circadian Clock of* Neurospora crassa: *Light-Induced Phase Shifting* (University of California, Santa Cruz, 1980).
27. Lakin-Thomas, P. L. Choline depletion, *frq* mutations, and temperature compensation of the circadian rhythm in *Neurospora crassa*. *J. Biol. Rhythms* **13,** 268–277 (1998).
28. Thresher, R. J. *et al.* Role of mouse cryptochrome blue-light photoreceptor in circadian photoresponses. *Science* **282,** 1490–1494 (1998).
29. Stanewsky, R. *et al.* The cry^{b} mutation identifies cryptochrome as a circadian photoreceptor in *Drosophila*. *Cell* **95,** 681–692 (1998).
30. Roenneberg, T. & Taylor, W. Automated Recordings of Bioluminescence—with special reference to the analysis of circadian rhythms. *Methods Enzymol.* **305** (in the press).

Acknowledgements. This work is dedicated to the memory of J. Aschoff. We thank V. Schiewe, A. Kohnert and G. Meyer for excellent technical assistance; the members of the Woody Hastings lab for comments on the manuscript; and the DFG, the Meyer-Struckmann-Stiftung and the Münchner Medizinische Wochenschrift for support.

Correspondence and requests for materials should be addressed to T.R. (e-mail: till.roenneberg@imp.med.uni-muenchen.de) or M.M. (e-mail: martha@imp.med.uni-muenchen.de).

Control of organ shape by a secreted metalloprotease in the nematode *Caenorhabditis elegans*

Robert Blelloch* & Judith Kimble†‡§

** Program in Cell and Molecular Biology, † Howard Hughes Medical Institute, and ‡ Departments of Biochemistry and Medical Genetics and Laboratory of Molecular Biology, University of Wisconsin-Madison, Madison, Wisconsin 53706, USA*

The molecular controls governing organ shape are poorly understood. In the nematode *Caenorhabditis elegans*, the gonad acquires a U-shape by the directed migration of a specialized 'leader' cell, which is located at the tip of the growing gonadal 'arm'[1]. The *gon-1* gene is essential for gonadal morphogenesis: in *gon-1* mutants, no arm elongation occurs and somatic gonadal structures are severely malformed[2]. Here we report that *gon-1* encodes a secreted protein with a metalloprotease domain and

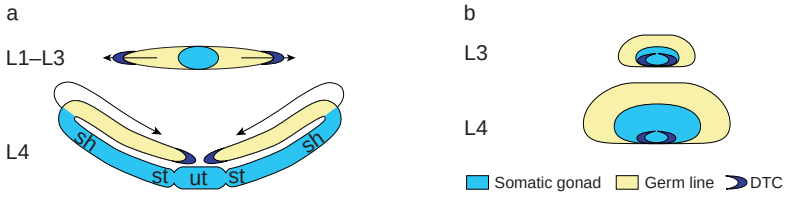

Figure 1 The *gon-1* gene is required for morphogenesis of the gonad. L1–L4, first to fourth larval stages. Arrows, direction of arm extension. **a**, Wild-type hermaphrodite. The gonad possesses two U-shaped ovotestes extending symmetrically from central gonadal structures that include uterus (ut), spermatheca (st) and sheath (sh). Hermaphrodite leader cells, called distal tip cells (DTCs) lead arm extension (for a review, see ref. 23). **b**, The *gon-1* gene is required for gonadal shape. In *gon-1* mutants, arm extension does not occur, and the gonad develops as a disorganized mass of somatic and germline tissues[2].

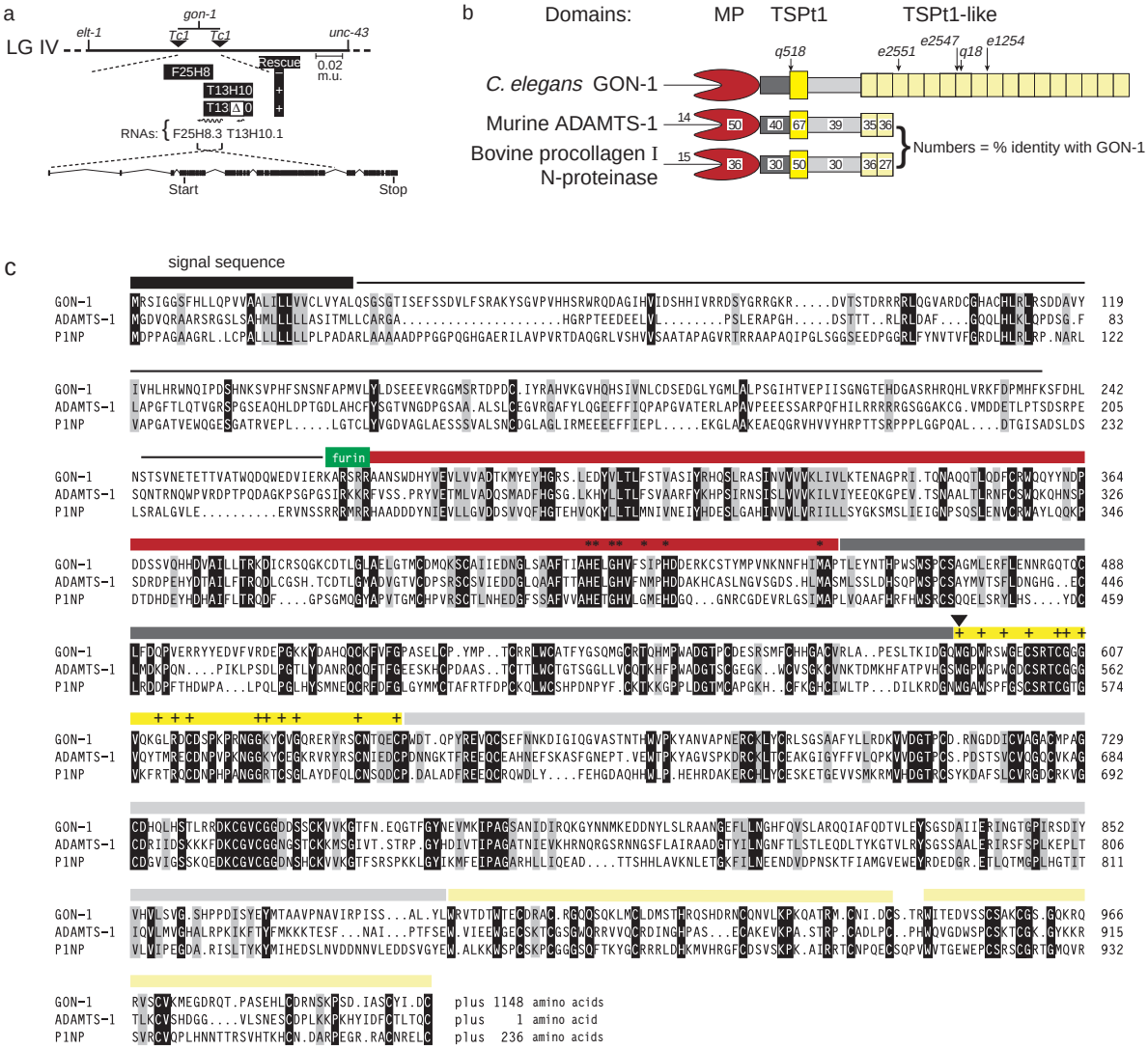

Figure 2 The *gon-1* gene and protein. **a**, Molecular cloning. Top, genetic map: *gon-1* maps to LG *IV* between Tc1 insertions pKP5151 and pKP614. Middle, *gon-1* transcript F25H8.3 spans two cosmids (F25H8 and T13H10); T13H10 rescues *gon-1*(*q518*), as does a deleted version that removes the smaller transcript T13H10.1. Below, the *gon-1* transcript, deduced by comparing genomic and cDNA sequences[24]. Black boxes, exons; translation start and stop sites are indicated. **b**, Domains of GON-1 and other family members. Prodomain, thin line; MP, metalloprotease (red); conserved cysteine-rich regions (CR1, dark grey) and CR2 (light grey); TSPt1, thrombospondin type 1 motif (bright yellow); TSPt1-like motifs, amino acids 889–1,923 (light yellow). Arrows, *gon-1* mutations: *q518* (TGG → TGA at amino acid 591), *e2551* (TGG → TAG at amino acid 1,069), *e2547* (TGG → TGA at amino acid 1,229), *q18* (TGG → TAG at amino acid 1,234) W → stop; *e1254* (CGA → TGA at amino acid 1,345) R → stop. **c**, GON-1 sequence alignment with two MPT family members. Colour coding as in **b**; black bar, predicted signal sequence; green bar, predicted furin-cleavage site. Black boxes, identical amino acids; grey boxes, similar amino acids. Alignment created by GCG Pileup program, with modification. In the metalloprotease domain (red), amino acids that are critical for enzymatic activity are marked by asterisks. In the TSPt1 domain, amino acids that are conserved in vertebrate TSPt1 repeats are marked by plus symbols. Filled triangle, site of *gon-1*(*q518*). Only the first two TSPt1-like motifs are shown; the consensus sequence for these repeats is W-X_{4-5}-W-X_2-CS-X_2-CG-X_{4-5}-X-G-X_3-R-X_3-C-X_{4-27}C-X_{8-12}-C-X_{3-4}-C.

multiple thrombospondin type-1-like repeats. This motif architecture is typical of a small family of genes that include bovine procollagen I N-protease (P1NP), which cleaves collagen[3], and murine ADAMTS-1, the expression of which correlates with tumour cell progression[4]. We find that *gon-1* is expressed in two sites, leader cells and muscle, and that expression in each site has a unique role in forming the gonad. We speculate that GON-1 controls morphogenesis by remodelling basement membranes and that regulation of its activity is crucial for achieving organ shape.

The *C. elegans* hermaphrodite gonad has two U-shaped arms that extend from the somatic gonadal structures (Fig. 1a). The shape of the male gonad is similar except that it has one arm. During gonadogenesis, elongation of the growing gonadal arms is controlled by leader cells[1], which are called distal tip cells (DTCs) in hermaphrodites and the linker cell (LC) in males. The *gon-1* gene is required for both elongation of the gonadal arms and morphogenesis of somatic gonadal structures[2] (Fig. 1b). To investigate *gon-1* function, we cloned the gene by a combination of genetic mapping, mutant rescue and RNA-mediated interference (Fig. 2a, legend). We confirmed the predicted gene F25H8.3 as *gon-1* by identifying molecular lesions in five *gon-1* mutant alleles (Fig. 2b, c; see below). The GON-1 protein bears a signal sequence at its amino terminus, but no predicted transmembrane domain, suggesting that it is secreted (Fig. 2c).

The GON-1 protein possesses a predicted metalloprotease (MP) domain (Fig. 2c, red bar) which is most similar to members of the reprolysin subfamily[5]. A potential furin cleavage site is located at the N-terminal border of the metalloprotease domain (Fig. 2c, green bar)[6,7]. GON-1 and the reprolysins share a common zinc-binding active site with the larger metzincin superfamily[8]. Amino-acid conservation within the active site, together with the known crystal structure of several superfamily members, reveals those amino acids that are essential for enzymatic activity (marked by asterisks in Fig. 2c)[8]. GON-1 has all amino acids implicated in catalysis and all but one implicated in structure of the active site. To test whether the GON-1 metalloprotease is essential for gene activity, we compared mutant rescue by one GON-1 transgene bearing the wild-type metalloprotease sequence to that of a second GON-1 transgene bearing a mutation at amino acid 425 within the active site. This mutation changes glutamic acid to alanine (E425A). In the metzincin family of metalloproteases, this mutation abolishes enzymatic activity without altering protein structure or stability[9,10]. The two transgenes were introduced at the same concentration into *gon-1* mutants, and rescue of arm extension was scored. The wild-type metalloprotease was capable of rescue (5/6 lines), whereas the mutant metalloprotease was not (0/16 lines). We conclude that GON-1 is an active metalloprotease and that metalloprotease activity is essential for its role in controlling morphogenesis.

In addition to its metalloprotease domain, GON-1 possesses a series of thrombospondin type 1 (TSPt1) repeats (Fig. 2b, c). The most N-terminal TSPt1 repeat bears the hallmarks of a canonical vertebrate TSPt1 repeat (15/16 of the consensus amino acids; + in Fig. 2c)[11], whereas the remaining 17 repeats are less similar and define a TSPt1-like variant. The function of the TSPt1 repeats was explored by analysing *gon-1* nonsense mutations predicted to remove varying numbers of repeats (Fig. 2b). One mutation, *gon-1*(*q518*), is in the canonical TSPt1 motif, and the others are in the TSPt1-like repeats. In *C. elegans*, mRNAs containing premature stop codons are normally degraded by the *smg* system, but, those mRNAs are stabilized in an *smg*-mutant background[12], the remaining activity of truncated GON-1 proteins should be evident in *smg-1*; *gon-1* double mutants. We found that *gon-1*(*q518*) was not suppressed in an *smg* background, whereas all four mutations in the TSPt1-like repeats (Fig. 2b) were suppressed (see Methods). Therefore, the GON-1(q518) mutant protein, which has the metalloprotease domain but not the bona fide TSPt1 motif or the rest of the C-terminal protein, is not capable of mutant rescue, but the other truncated proteins are. We infer that the region spanning from the TSPt1 motif to the second TSPt1-like motif is critical for GON-1 activity. We confirmed that two TSPt1-like repeats are sufficient for rescuing activity by mutant rescue with a mini-transgene (see below).

To determine where and when GON-1 is expressed during development, we generated a transgene, called *gon-1* 5′::GFP, carrying a predicted *gon-1* promoter fused to the coding region for green fluorescent protein (GFP). *gon-1* 5′::GFP drives GFP expression in the leader cells of both hermaphrodites and males during the period of most active gonadal-arm elongation (Fig. 3). In hermaphrodites, GFP is not observed in gonads from first-stage (L1) larvae (Fig. 3a, b). Its first gonadal expression occurs in L2 and is limited to the DTCs (Fig. 3c, d). GFP continues to be expressed in DTCs through L4 (Fig. 3e, f), but is faint or not detectable in the adult (Fig. 3g, h). GFP is similarly expressed in the male linker cell (Fig. 3i, j; data not shown). In addition to its expression in leader cells, the *gon-1* promoter also drives GFP in muscle cells throughout development (Fig. 3k; data not shown).

To explore the significance of *gon-1* expression in leader cells and in muscle, we placed *gon-1* coding sequences under the control of either of two heterologous promoters. The *lag-2* promoter drives expression in the hermaphrodite DTC[13], whereas the *unc-54* promoter drives expression in body-wall muscle[14]. For both transgenes, effects were examined in a *gon-1* null (*0*) background. We found that *lag-2* 5′::GON-1 rescues arm extension and fertility (5/6 lines) (Fig. 4c), but *unc-54 5′*::GON-1 does not (0/11 lines). However, *unc-54 5′*::GON-1 does affect gonadal shape. Whereas the gonadal tissues of *gon-1* mutants are not consolidated in a single mass (Fig. 4b), those of *gon-1(0)*; *unc-54* 5′::GON-1 form a discrete mass that

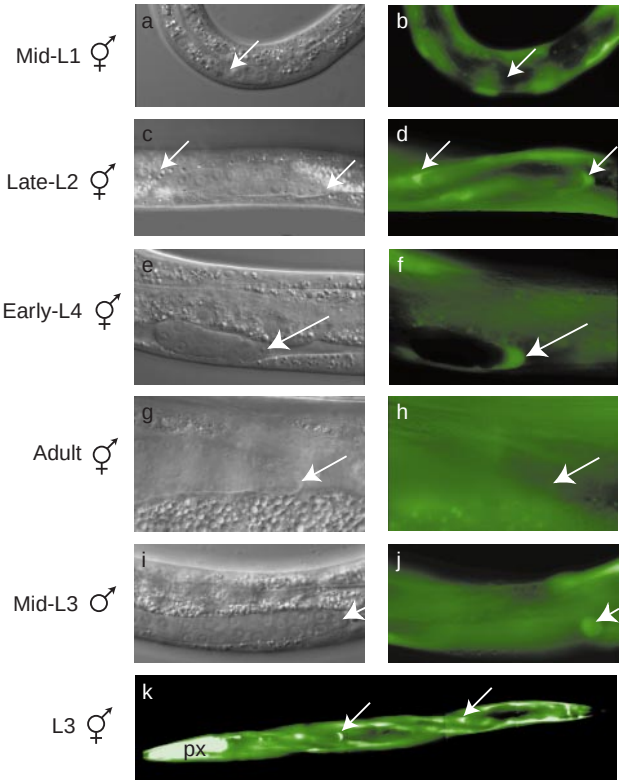

Figure 3 The *gon-1* promoter drives GFP expression in leader cells and in muscle. All animals are wild type and carry *gon-1* 5′::GFP. **a**, **c**, **e**, **f**, **h**, Nomarski; **b**, **d**, **f**, **g**, **i**, GFP fluorescence. Same animal in each left–right pair. Arrows, leader cells. **a**, **b**, No GFP in early gonad (arrow, progenitor of leader cell). **c–f**, GFP is expressed in leader cells during active elongation. **g**, **h**, GFP is not expressed in adult leader cell. **i**, **j**, Male leader cell expresses GFP. **k**, GFP is expressed in all muscles as well as in the leader cells. Body wall muscle extends length of body in four stripes, which are twisted because of the roller phenotype (see Methods). px, Pharynx; arrows, DTCs.

is expanded in all axes (Fig. 4d). Therefore, muscle expression of *gon-1* permits the contained growth and expansion of gonadal tissues within a basement membrane. Furthermore, because GON-1 expressed in muscle can act non-autonomously on the gonad, we conclude that GON-1 is secreted and can act over a distance. We propose that, in wild-type animals, *gon-1* must be expressed in leader cells to achieve a localized activity that directs elongation of gonadal arms along the proximal–distal axis. In addition, *gon-1* expression in muscle may provide a diffuse activity that is important for expansion of the gonad along dorsal–ventral and left–right axes. By this model, the combination of localized and dispersed activities is important in defining the final shape of the organ.

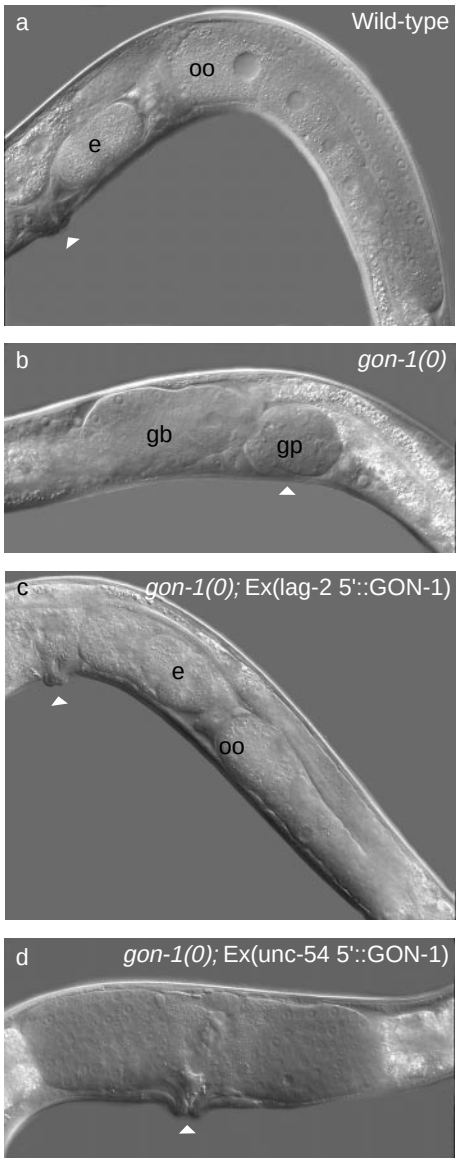

Figure 4 *gon-1* expression is critical for organ shape. **a–d**, Differential interference contrast (DIC) microscopy of adult hermaphrodites. Solid triangle, vulva; e, embryo; oo, oocyte. **a**, Wild type. Gonadal arm has normal U-shape. **b**, *gon-1(0)*. No arm extension and gonadal tissues are irregularly shaped. gp, gonad proper; gb, gonadal tissue bulging from gp. **c**, *gon-1(0)* with *gon-1(+)* expressed in DTC. Gonad can develop with U-shaped arm. Some animals are fertile, but more commonly, somatic gonadal structures (for example, uterus) are poorly formed and animals are sterile. Furthermore, the distal gonadal arms are thinner than normal. **d**, *gon-1(0)* with *gon-1(+)* expressed in body wall muscle. Gondal tissue is more coherent than in *gon-1* mutants and has expanded in all three axes.

We suggest that the GON-1 metalloprotease permits and directs expansion of the gonad by remodelling the basement membrane. GON-1 belongs to a small gene family of secreted metalloproteases with one canonical TSPt1 domain, multiple TSPt1-like motifs and two conserved cysteine-rich regions (Fig. 2b). Based on this conserved architecture, we suggest the name MPT (for MetalloProtease with TSPt1 repeats) for the family. Bovine P1NP can proteolyse the N-terminal propeptide from collagen I (refs 3, 15). We show that metalloprotease activity is required for GON-1 function and propose that, like P1NP, it may cleave components of the extracellular matrix. Murine expression of *adamts-1* RNA correlates with tumour cell progression[4]. Given the role of GON-1 in promoting cell migration of the *C. elegans* leader cell, we suggest that MPT proteins may be involved more generally in cell migrations that must pass through extracellular matrix and that, in cancerous tissues, a change in MPT regulation may promote metastasis.

The GON-1 metalloprotease drives arm extension during gonadogenesis in *C. elegans*, and localization of its activity has a profound effect on organ shape. We suggest that similar activities may control organ morphogenesis throughout the animal kingdom, and previous *in vitro* experiments support this notion. For example, antibodies recognizing matrix metalloprotease 9 (MMP9) can block branching of the ureter bud during kidney development[16], and inhibitors of MMPs block the invasion of endothelial cells into a fibrin matrix in assays for angiogenesis[17]. Based on these observations and our analysis of GON-1, we suggest that the matrix metalloproteases are critical modulators of organogenesis. With the identification of GON-1 in *C. elegans*, the functions of MPT metalloproteases can be analysed *in vivo* during organogenesis using the full force of molecular genetics available in this model system. □

Methods

Mapping and rescue of *gon-1*. Four-factor mapping placed *gon-1* between Tc1 insertions pKP614 and pKP5151. Specifically, two out of ten fertile Unc recombinants from *unc-24 gon-1 dpy-20/pKP5151* mothers did not carry the Tc1, placing *gon-1* right of pKP5151. One of 52 fertile Dpy recombinants from *unc-24 gon-1 dpy-20/pKP614* was negative for the Tc1, placing *gon-1* left of pKP614. Tc1 insertions were scored by polymerase chain reaction (PCR) as previously described[18]. For rescue experiments, 10 μg ml^{-1} cosmid plus 100 μg ml^{-1} pRF4 were co-injected into *unc24 gon-1/gon-4 dpy-20* as described previously[19]. From 13 F1 roller lines injected with the T13H10 cosmid, we identified 3 rescued fertile Unc progeny. pJK651 (a deleted version of T13H10), was constructed by digesting with *Kpn*I and religating the backbone. pJK651 rescued at a similar efficiency as T13H10. RNA-mediated interference (RNAi) was performed with both single-stranded and double-stranded RNA. Approximately 2 mg ml^{-1} RNA corresponding to a 1 kilobase (kb) portion of each predicted transcript on T13H10 were injected into N2 gonads as described[20]. Phenocopy was scored as absence of DTC migration. Molecular lesions were identified by direct sequencing of PCR products spanning the *gon-1* gene from single-mutant worms[21]. Sequencing was done on an ABI sequencer. Complementary DNAs were isolated from the following libraries: λRB1 and λRB2 (gifts from R. Barstead) and λAE.1 (gift from A. Puoti). cDNAs spanning the remaining gaps were isolated by performing PCR after reverse transcription of RNA[22]. The 5′ end was identified using an SL1-specific primer and nested primers within the predicted transcript[22]. For *gon-1*; *smg-1* double mutants, non-Unc progeny from *gon-1/nT1[unc-?(n754 dm) let-?)]*; *smg-1(r861)* mothers were isolated and scored for fertility and arm extension. *nT1[unc-?(n754 dm) let-?)]* is a dominant Unc balancer for *gon-1*.

Transgene experiments. To construct *gon-1* 5′::GFP, we performed Expand High-Fidelity PCR (Boehringer Mannheim) with restriction-site-tagged primers that spanned −7 to −11,547 relative to the initiator ATG of the *gon-1* genomic DNA sequence. This region contains 4 kb of *gon-1* 5′ flanking region and 8 kb of the *gon-1* transcribed region preceding the first AUG (two large introns, one small intron and the 500 nucleotides of 5′UTR (Fig. 2a)). All PCR reactions used pJK561 as template. The *gon-1* 5′ PCR product was cloned into the pPD95.77 vector (from A. Fire). The resulting *gon-1* 5′::GFP construct was co-injected at 5 μg ml^{-1} with pRF4 (100 μg ml^{-1}). Stably transmitting roller

lines were scored for fluorescence. To construct the *gon-1*(+) minigene, we performed high-fidelity PCR with restriction-site-tagged primers spanning −7 to +5,276 of *gon-1* gDNA. To construct the *gon-1* (E → A) mutant minigene, we made primers that introduced a T-to-G mutation at +2,546 and an A-to-C mutation at +2,551. The first mutation is translationally silent and introduces a *Sph*I restriction site whereas the second mutation causes an E-to-A transition in the GON-1 metalloprotease active site. We used these primers to amplify either half of the wild-type minigene and spliced the resulting products using the new *Sph*I site. Sequencing of *gon-1*(+) and *gon-1*(E → A) showed no second-site mutations. The two minigenes were cloned into pPD49.26 (from A. Fire) together with the *lag-2* 5′ promoter from pJK375 (ref. 13). The *lag-2* 5′::GON-1(+) and *lag-2* 5′::GON-1(E → A) constructs were injected at 1 μg ml^{-1} together with pRF4 (50 μg ml^{-1}) into *unc-24*(*e138*) *gon-1*(*q518*)/*gon-4*(*e2575*) *dpy-20*(*e1282*) hermaphrodites. Roller Unc animals from stably transmitting roller lines were scored for arm extension and fertility in both F2 and F3 generations. The *unc-54*::GON-1(+) transgene was constructed by cutting the *gon-1*(+) minigene from *lag-2* 5′::GON-1(+) and splicing it downstream of the *unc-54* promoter in pPD30.35 (from A. Fire). The resulting transgene was co-injected at both 1 μg ml^{-1} (50 μg ml^{-1} pRF4) and 5 μg ml^{-1} (100 μg ml^{-1} pRF4) into *gon-1* heterozygotes and scored as above. Effects on *gon-1* gonadal structure were mild at 1 μg ml^{-1} and stronger at 5 μg ml^{-1}.

Received 24 March; accepted 27 April 1999.

1. Kimble, J. E. & White, J. G. On the control of germ cell development in *Caenorhabditis elegans*. *Dev. Biol.* **81,** 208–219 (1981).
2. Blelloch, R., Santa Anna-Arriola, S., Li, Y., Hodgkin, J. & Kimble, J. The *gon-1* gene regulates morphogenesis of the *C. elegans* gonad (submitted).
3. Colige, A. *et al.* cDNA cloning and expression of bovine procollagen I N-proteinase: a new member of the superfamily of zinc-metalloproteinases with binding sites for cells and other matrix components. *Proc. Natl Acad. Sci. USA* **94,** 2374–2379 (1997).
4. Kuno, K. *et al.* Molecular cloning of a gene encoding a new type of metalloproteinase-disintegrin family protein with thrombospondin motifs as an inflammation associated gene. *J. Biol. Chem.* **272,** 556–562 (1997).
5. Rawlings, N. D. & Barrett, A. J. Evolutionary families of metallopeptidases. *Methods Enzymol.* **248,** 183–228 (1995).
6. Pei, D. & Weiss, S. J. Furin-dependent intracellular activation of the human stromelysin-3 zymogen. *Nature* **375,** 244–247 (1995).
7. Pei, D. & Weiss, S. J. Transmembrane-deletion mutants of the membrane-type matrix metalloproteinase-1 process progelatinase A and express intrinsic matrix-degrading activity. *J. Biol. Chem.* **271,** 9135–9140 (1996).
8. Stöcker, W. *et al.* The metzincins—topological and sequential relations between the astacins, adamalysins, serralysins, and matrixins (collagenases) define a superfamily of zinc-peptidases. *Protein Sci.* **4,** 823–840 (1995).
9. Cha, J. & Auld, D. S. Site-directed mutagenesis of the active site glutamate in human matrilysin: investigation of its role in catalysis. *Biochemistry* **36,** 16019–16024 (1997).
10. Will, H., Atkinson, S. J., Butler, G. S., Smith, B. & Murphy, G. The soluble catalytic domain of membrane type 1 matrix metalloproteinase cleaves the propeptide of progelatinase A and initiates autoproteolytic activation. *J. Biol. Chem.* **271,** 17119–17123 (1996).
11. Adams, J. C., Tucker, P. R. & Lawler, J. *The Thrombospondin Gene Family* (Landes, Austin, Texas, 1995).
12. Anderson, P. & Kimble, J. in *C. elegans* II (eds Riddle, D. L., Blumenthal, T., Meyer, B. J. & Priess, J. R.) 185–208 (Cold Spring Harbor Laboratory Press, 1997).
13. Henderson, S. T., Gao, D., Lambie, E. J. & Kimble, J. *lag-2* may encode a signaling ligand for the GLP-1 and LIN-12 receptors of *C. elegans*. *Development* **120,** 2913–2924 (1994).
14. Okkema, P. G., Harrison, S. W., Plunger, V., Aryana, A. & Fire, A. Sequence requirements for myosin gene expression and regulation in *Caenorhabditis elegans*. *Genetics* **135,** 385–404 (1993).
15. Colige, A. *et al.* Characterization and partial amino acid sequencing of a 107-kDa procollagen I *N*-proteinase purified by affinity chromatography on immobilized type XIV collagen. *J. Biol. Chem.* **270,** 16724–16730 (1995).
16. Lelongt, B., Trugnan, G., Murphy, G. & Ronco, P. M. Matrix metalloproteinases MMP2 and MMP9 are produced in early stages of kidney morphogenesis but only MMP9 is required for renal organogenesis in vitro. *J. Cell Biol.* **136,** 1363–1373 (1997).
17. Hiraoka, N., Allen, E., Apel, I. J., Gyetko, M. R. & Weiss, S. J. Matrix metalloproteinases regulate neovascularization by acting as pericellular fibrinolysins. *Cell* **95,** 365–377 (1998).
18. Korswagen, H. C., Durbin, R. M., Smits, M. T. & lasterk, R. H. A. Transposon Tc1-derived, sequence-tagged sites in *Caenorhabditis elegans* as markers for gene mapping. *Proc. Natl Acad. Sci. USA* **93,** 14680–14685 (1996).
19. Mello, C. & Fire, A. in *Caenorhabditis elegans: Modern Biological Analysis of an Organism* (eds Epstein, H. F. & Shakes, D. C.) 451–482 (Academic, New York, 1995).
20. Fire, A. *et al.* Potent and specific genetic interference by double-stranded RNA in *Caenorhabditis elegans*. *Nature* **391,** 806–811 (1998).
21. Williams, B. D., Schrank, B., Huynh, C., Shownkeen, R. & Waterston, R. H. A genetic mapping system in Caenorhabditis elegans based on polymorphic sequence-tagged sites. *Genetics* **131,** 609–624 (1992).
22. Krause, M. in *Caenorhabditis elegans: Modern Biological Analysis of an Organism* (eds Epstein, H. F. & Shakes, D. C.) 513–533 (Academic, New York, 1995).
23. Schedl, T. in *C. elegans* II (eds Riddle, D. L., Blumenthal, T., Meyer, B. J. & Priess, J. R.) 241–269 (Cold Spring Harbor Laboratory Press, 1997).
24. The *C. elegans* Sequencing Consortium. Genome sequence of the nematode *C. elegans*: a platform for investigating biology. *Science* **282,** 2012–2018 (1998).

Acknowledgements. We thank A. Coulson for providing cosmids, R. Barstead and A. Puoti for cDNA libraries, A. Fire for GFP and expression vectors, D. Gao for *lag-2* promoter, J. Nance for Tc1 primers, the Caenorhabditis Genetics Center for worm strains, and the many lab members who provided thoughts and criticisms during the course of this work. R.B. is an MD/PhD student and was an NIH Molecular Biosciences trainee. J.K. is an investigator with the Howard Hughes Medical Institute and has been supported by grants from NIH and NSF.

Correspondence and requests for materials should be addressed to J.K. (e-mail: jekimble@facstaff.wisc.edu).

Emergence of vancomycin tolerance in *Streptococcus pneumoniae*

R. Novak*, B. Henriques†, E. Charpentier*, S. Normark† & E. Tuomanen*

** Dept of Infectious Diseases, St. Jude Children's Research Hospital, 332 N. Lauderdale St., Memphis, Tennessee 38105, USA*
† Swedish Institute for Infectious Disease Control, Karolinska Institute, S171-82 Solna, Stockholm, Sweden

***Streptococcus pneumoniae*, the pneumococcus, is the most common cause of sepsis and meningitis[1]. Multiple-antibiotic-resistant strains are widespread, and vancomycin is the antibiotic of last resort[2,3]. Emergence of vancomycin resistance in this community-acquired bacterium would be catastrophic. Antibiotic tolerance, the ability of bacteria to survive but not grow in the presence of antibiotics, is a precursor phenotype to resistance[4]. Here we show that loss of function of the VncS histidine kinase of a two-component sensor-regulator system in *S. pneumoniae* produced tolerance to vancomycin and other classes of antibiotic. Bacterial two-component systems monitor environmental parameters through a sensor histidine-kinase/phosphatase, which phosphorylates/dephosphorylates a response regulator that in turn mediates changes in gene expression. These results indicate that signal transduction is critical for the bactericidal activity of antibiotics. Experimental meningitis caused by the *vncS* mutant failed to respond to vancomycin. Clinical isolates tolerant to vancomycin were identified and DNA sequencing revealed nucleotide alterations in *vncS*. We conclude that broad antibiotic tolerance of *S. pneumoniae* has emerged in the community by a molecular mechanism that eliminates sensitivity to the current cornerstone of therapy, vancomycin.**

The bactericidal activity of antibiotics that stop cell-wall synthesis relies on activation of bacterially encoded death effectors[4–6]. In pneumococcus, the autolysin protein LytA serves this function and is triggered by antibiotics to digest the cell-wall exoskeleton[4]. The autolysins of all bacteria, including the pneumococcal LytA, are presumed to be under strong negative regulation as they are constitutively produced, potentially suicidal and physiologically activated in stationary phase[6]. The mechanism of their activation is unknown and is an important question in basic microbiology. To define elements in the autolysin trigger pathway, we searched for loss of penicillin-induced autolysis in a library of pneumococcal

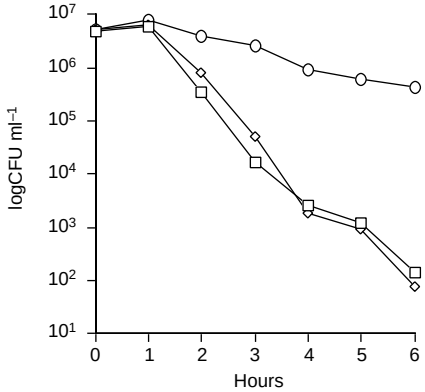

Figure 1 Effect of loss of function of *vncR* and *vncS* on bactericidal activity of vancomycin. Wild-type strain R6 (squares), *vncR* mutant (diamonds) and *vncS* mutant (circles). Cultures in the early exponential phase of growth (10^7 CFU ml^{-1}) were treated with 10 × the MIC of vancomycin (5 μg ml^{-1}), and bacterial viability was followed for 6 h.